

# H.K. Moffatt

## High frequency excitation of liquid metal systems

*Department of Applied Mathematics and  
Theoretical Physics, University of Cambridge*

### ABSTRACT

*If a container of liquid metal, which may be wholly or partly filled, is placed in a high frequency magnetic field (either single-phase or multiphase) of external origin, the induced currents are confined to a thin surface layer within which vorticity is generated. By integration of the equation of motion through this layer, it is shown that the net effect of the Lorentz force is to induce an effective surface velocity just inside the surface layer on a rigid boundary, and an effective surface stress just inside the layer on a free surface. These effects can be very strong in the neighbourhood of any sharp corners on the fluid boundary where the magnetic pressure is unbounded in the high frequency limit. The local electrodynamic and fluid dynamical behaviour in such corner regions is analysed in detail, with particular attention to the cases of single-phase fields and rotating fields. When the Reynolds number is large, a boundary-layer description of the driven flow is appropriate, and similarity solutions of Falkner-Skan type are obtained, both for the case when the boundaries are rigid and for the case when a sharp crest forms on a free surface. The relevance of these solutions in practical contexts is discussed.*

### 1. INTRODUCTION

Alternating magnetic fields are used in a wide variety of practical contexts to generate and control the motion of liquid metals. For example, single-phase a.c. fields are used in the induction furnace /1, 2/, the primary function of the field being the Joule heating effect, but a vital secondary function being the transport of heat by the motion driven by the Lorentz force distribution. Single-phase fields are also used in the shaping of liquid metal extrusions /3/, the surface being a free surface whose shape is controlled by the distribution of magnetic

pressure; this generally non-uniform magnetic pressure is necessarily accompanied by a generation of vorticity in the magnetic boundary layer (or skin) in the fluid, to which the a.c. field is confined. The resulting flow reacts back, via dynamic pressures, on the shape of the free surface, and therefore solution of the shape problem generally requires an understanding of the interior flow. The same type of interactive situation occurs in the magnetic levitation problem /4, 5/ in which the magnetic pressure distribution over the surface of a sample of liquid metal is used to support the sample against gravity, as well as to control its shape.

Multiphase fields, and in particular rotating fields, are used to generate rotation of liquid metal in confined regions /6-8/. This process has been studied particularly in the context of continuous casting of steel, where it is known that stirring helps to prevent the formation of dendritic structures and thus to yield a better final product. The simple theory of the effect of a rotating field on fluid contained in a cylinder of circular cross-section was described in Ref. 9, and a number of more complicated geometries have been studied (for a review, see Ref. /10/).

In the present paper, we aim to synthesise some of these studies, to place them in a general framework, and to study particularly the important effects that can arise near sharp corners in the fluid boundary. When the field frequency  $\omega$  is high (and this is the situation to which we shall limit attention) the corners become particularly important because the field and the magnetic pressure become singular at the corners, and it becomes necessary to understand the local properties of the flow that results.

In Section 2, we provide a general analysis of the "skin dynamics", and we show that the net effect of the a.c. field is to replace the no-slip condition at a rigid boundary  $S$  by the prescription of an "induced tangential velocity"  $u_s$ , determined by the local properties of the magnetic field. Similarly it is shown in Section 3 that at a free surface  $\Gamma$ , the usual condition of zero tangential stress

is replaced by a condition of prescribed "induced tangential stress"  $\tau_T$ , again determined by the local field structure.

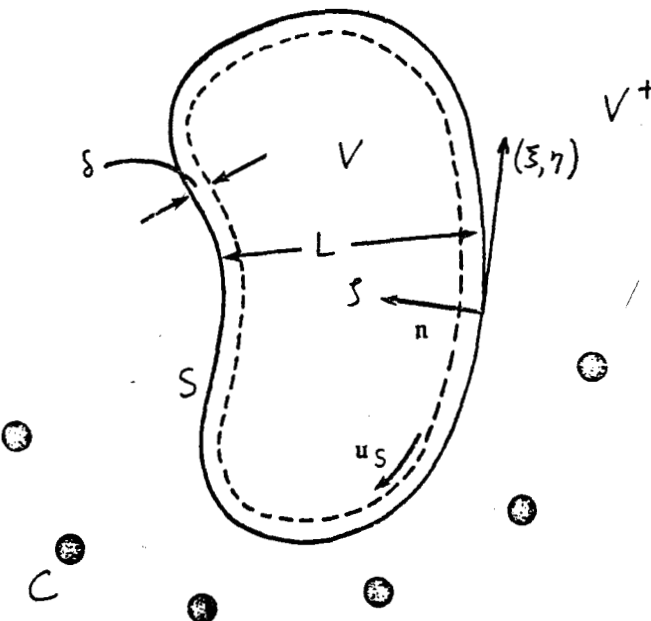
In Section 4, conditions near a sharp corner between two rigid boundaries are analysed both for single phase and multiphase fields, and low Reynolds number solutions are presented. In Section 5, the high Reynolds number situation is explored, and similarity solutions of Falkner-Skan type are presented, where these are applicable. In Section 6, the behaviour near a contact line between a free surface and a rigid boundary is discussed, and in Section 7 the possible behaviour near a sharp crest on a free surface is investigated. Finally, in Section 8 we discuss the limitations of the analysis and the extent to which the results may be relevant in practical contexts.

## 2. INDUCED VELOCITY AT A RIGID INSULATING BOUNDARY

We consider first the configuration sketched in Fig. 1: liquid metal occupies the region  $V$  bounded by the rigid, electrically insulating, closed surface  $S$ . The exterior region is denoted  $V^+$ . Alternating currents flow in coils  $C$  which lie in  $V^+$ ; these give rise to a magnetic field  $\text{Re}(\mathbf{B}(\mathbf{x})e^{i\omega t})$  which penetrates a distance  $O(\delta)$  into  $V$ , where

$$\delta = (2\mu_0\sigma\omega)^{-1/2} \quad (2.1)$$

$\sigma$  being the electrical conductivity of the fluid;  $\delta$  is of course the familiar skin thickness. We suppose that  $\omega$  is large so that  $\delta$  is small compared with the typical dimension  $L$  of  $V$ ; indeed we shall suppose that  $\delta$  is small



1 Configuration sketch: liquid metal is contained within insulating boundary  $S$ ; ac currents flow in external coils  $C$ ;  $\delta$  is skin thickness, and  $u_s$  is induced surface velocity just inside skin

compared with any other length scales (e.g. viscous boundary-layer thicknesses) that may arise in the analysis.

To leading order, the field in  $V^+$  may then be determined from solution of the potential problem

$$\left. \begin{aligned} \mathbf{B}^+(\mathbf{x}) &= \nabla\Phi, \quad \nabla^2\Phi = 0 \quad \text{in } V^+ \\ \mathbf{B}^+ \cdot \mathbf{n} &= \partial\Phi/\partial n = 0 \quad \text{on } S \end{aligned} \right\} \quad (2.2)$$

where  $\mathbf{n}$  is the unit normal on  $S$  into  $V$ ; moreover,  $\Phi$  has singularities prescribed by the magnitude of the currents in the exciting coils. If all these currents are in phase, then  $\Phi(\mathbf{x})$  may be taken to be real; but if the applied currents are not all in phase (as for example in the rotating field problem) then  $\Phi$  is complex, i.e.

$$\Phi = \Phi^{(r)}(\mathbf{x}) + i\Phi^{(i)}(\mathbf{x}) \quad (2.3)$$

where  $\nabla\Phi^{(i)}$  is not generally parallel to  $\nabla\Phi^{(r)}$ . The field on  $S$ ,  $\mathbf{B}_S(\mathbf{x})$  is tangential to  $S$ , i.e.  $\mathbf{n} \cdot \mathbf{B}_S = 0$ . Note however that since

$$(\nabla \cdot \mathbf{B})_{x \in S} = \nabla \cdot \mathbf{B}_S + \partial B_n / \partial n = 0$$

the two-dimensional divergence of  $\mathbf{B}_S$  is not zero; in fact,

$$\nabla \cdot \mathbf{B}_S = -\partial B_n^+ / \partial n = -\partial^2 \Phi / \partial n^2 |_S \quad (2.4)$$

Let us now choose local Cartesian coordinates  $O\xi\eta\zeta$ , with  $O\zeta$  directed along  $\mathbf{n}$  (so that  $\partial/\partial\zeta \equiv \partial/\partial n$ ) and  $O\xi$ ,  $O\eta$  in the tangent plane. Then the usual theory of the skin-effect gives for the field  $\mathbf{B}(\mathbf{x})$  in  $V$ ,

$$\mathbf{B} = (\mathbf{B}_S(\xi, \eta) + \mathbf{B}_\zeta(\xi, \eta)\mathbf{n})e^{-(1+i)\zeta/\delta}e^{i\omega t} \quad (2.5)$$

(real part understood). Here the weak normal component  $\mathbf{B}_\zeta$  is determined by the condition  $\nabla \cdot \mathbf{B} = 0$  so that

$$-\frac{(1+i)}{\delta}\mathbf{B}_\zeta = -\nabla \cdot \mathbf{B}_S = \frac{\partial^2 \Phi}{\partial n^2} |_S \quad \text{from (2.4)} \quad (2.6)$$

The current  $\mathbf{J}$  in the skin is given (to leading order) by

$$\begin{aligned} \mu_0 \mathbf{J} &= \nabla \times \mathbf{B} \approx -\delta^{-1}(1+i)(\mathbf{n} \times \mathbf{B}_S) \times \\ &\times e^{-(1+i)\zeta/\delta}e^{i\omega t} \end{aligned} \quad (2.7)$$

and the mean Lorentz force in the layer is then given by  $\mathbf{F} = \frac{1}{2}\text{Re}(\mathbf{J}^* \times \mathbf{B})$ ; using (2.5)–(2.7), this simplifies to

$$\mathbf{F} = (2\mu_0\delta)^{-1} [|\mathbf{B}_S|^2 \mathbf{n} - \delta \text{Im} \mathbf{B}_S^* (\nabla \cdot \mathbf{B}_S)] e^{-2\zeta/\delta} \quad (2.8)^\dagger$$

This force is predominantly normal to  $S$ , and the smaller tangential component arises only in the multiphase situation (when  $\mathbf{B}_S$  is complex). However, it is really the curl of  $\mathbf{F}$  that generates flow, and the two terms contributing

<sup>†</sup> A similar result was first obtained by Sneyd (Ref. /10/).

to  $F$  in (2.8) are generally equally effective in driving the flow (see below).

Consider first the motion that is driven by the force field  $F(x)$  in the layer in which  $\zeta = O(\delta)$ . A lubrication-type approximation is clearly legitimate, i.e.

$$\nu \partial^2 u / \partial \zeta^2 \approx \nabla P - p^{-1} F \quad \text{for } |\zeta| = O(\delta) \quad (2.9)$$

where  $P = p/\rho - g \cdot x$ ,  $p$  is the pressure field within the layer,  $u$  the velocity field,  $\rho$  the density and  $\nu$  the kinematic viscosity of the fluid. The normal component of (2.9) (under this approximation) is

$$\partial P / \partial \zeta \approx p^{-1} F \cdot n = (2\rho\mu_0\delta)^{-1} |B_S^2| e^{-2\zeta/\delta} \quad (2.10)$$

Hence

$$P = P_0(\zeta, \eta) - (4\mu_0\rho)^{-1} |B_S^2| e^{-2\zeta/\delta} \quad (2.11)$$

where  $P_0(\zeta, \eta)$  is the "pressure" distribution that is established inside the skin, i.e. for  $\zeta \gg \delta$ . Substitution in (2.9) now gives the tangential equation

$$\nu \partial^2 u / \partial \zeta^2 \approx \nabla P_0 - \frac{1}{2} Q(x) e^{-2\zeta/\delta} \quad (2.12)$$

where  $Q(x)$  is a vector field with the dimensions of an acceleration defined on  $S$  (and tangent to  $S$ ) given by

$$Q(x) = (\mu_0\rho)^{-1} [ \frac{1}{2} |B_S|^2 - \text{Im} B_S^* \nabla \cdot B_S ] \quad (2.13)$$

It seems clear that the term  $\nabla P_0$  in (2.12) should be negligible within the layer  $\zeta = O(\delta)$  provided  $\delta$  is small enough. Let us suppose that this is the case, and check for consistency in retrospect. The solution of (2.12) satisfying  $u = 0$  on  $z = 0$  is then

$$u = -\frac{1}{8} \delta^2 \nu^{-1} Q(x) (e^{-2\zeta/\delta} - 1) \quad (2.14)$$

and asymptotically,

$$u \sim \frac{1}{8} \delta^2 \nu^{-1} Q(x) \quad \text{for } \zeta \gg \delta \quad (2.15)$$

Let  $Q_0$  be a typical magnitude of  $|Q(x)|$ . Then the velocity scale determined by (2.15) is

$$U \sim \delta^2 \nu^{-1} Q_0 \quad (2.16)$$

and the associated Reynolds number is

$$\text{Re} = UL/\nu = \delta^2 L \nu^{-2} Q_0 \quad (2.17)$$

We shall suppose that  $\text{Re} \gg 1$ , the situation of greatest practical interest. The interior pressure gradients then have order of magnitude  $\rho U^2/L$ , and so

$$|\nabla P_0| \sim U^2/L \quad (2.18)$$

Hence

$$|\nabla P_0|/Q \sim \text{Re} (\delta/L)^2 \quad (2.19)$$

and so the term  $\nabla P_0$  in (2.12) is indeed negligible provided

$$(\delta/L)^2 \ll \text{Re}^{-1} \ll 1 \quad (2.20)$$

As far as the interior flow is concerned, therefore, the net effect of the rotational force within the skin is to generate an effective tangential velocity, which we shall describe as the induced surface velocity

$$u_S = \frac{1}{8} \delta^2 \nu^{-1} Q(x) \quad \text{on } S, \quad (2.21)$$

where  $Q(x)$  is given by (2.13). All the electromagnetic effects are contained within this formula. The problem that remains is the purely fluid mechanical one of determining the flow in  $V$  subject to the prescribed velocity  $u = u_S$  on  $S$ .

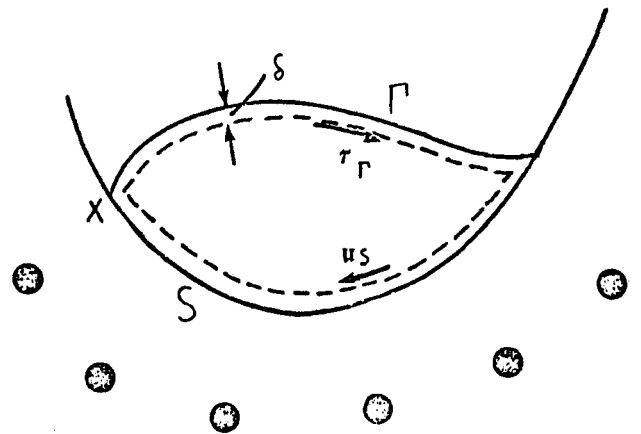
### 3. INDUCED TANGENTIAL STRESS AT A FREE SURFACE

Let us now consider the modifications required in the above description if part (or all) of the fluid boundary is a free surface (Fig. 2); we denote this part of the boundary by  $\Gamma$  (and  $S$  will continue to denote the rigid boundary part). The shape of  $\Gamma$  is controlled by the normal stress condition

$$(2\mu_0)^{-1} |B_S|^2 - \rho g \cdot x + \gamma \kappa = \text{cst. on } \Gamma \quad (3.1)$$

where  $\gamma$  is the surface tension and  $\kappa$  the surface curvature. Equivalently, there is a variational principle for the determination of the position of  $\Gamma$ , viz.

$$W \equiv W_g + W_\gamma - W_M \quad (3.2)$$



2 Configuration sketch when fluid is bounded partly by free surface  $\Gamma$  (situation in neighbourhood of contact line  $X$  is considered in § 6). Inside skin on  $\Gamma$  there is induced surface stress  $\tau_\Gamma$

is stationary (and in fact minimal) with respect to small variations in  $\Gamma$  from its equilibrium position, where

$$W_g = - \int_V \rho g \cdot x \, dV = \text{gravitational energy} \quad (3.3)$$

$$W_\gamma = \gamma A_\Gamma = \text{surface tension energy} \quad (A_\Gamma = \text{area of } \Gamma) \quad (3.4)$$

$$W_M = \int_V + (4\mu_0)^{-1} |B|^2 \, dV = \text{mean magnetic energy} \quad (3.5)$$

Just as in Section 2, there is an electromagnetic skin on  $\Gamma$  within which a thin film approximation is applicable, and all the equations up to (2.13) are still valid. Now however the argument for the neglect of  $\rho^{-1} \nabla P_0$  is a little modified. If we neglect  $\rho^{-1} \nabla P_0$  in (2.12), and integrate once using the condition of zero tangential stress  $\partial u / \partial \xi = 0$  on  $\xi = 0$ , we obtain

$$\partial u / \partial \xi = \frac{1}{4} \delta \nu^{-1} Q(x) (e^{-2\xi/\delta} - 1) \quad (3.6)$$

so that

$$\partial u / \partial \xi \sim -\frac{1}{4} \delta \nu^{-1} Q(x) \quad \text{for } \xi \gg \delta. \quad (3.7)$$

This velocity *gradient* becomes the prescribed *outer* condition for the interior flow; and the associated velocity scale is now

$$U_1 \sim \delta \nu^{-1} Q_0 L = (L/\delta) U. \quad (3.8)$$

The order of magnitude of  $\nabla P_0$  (cf. (2.18)) is now  $|\nabla P_0| \sim U_1^2/L$ , and so

$$|\nabla P_0| / |\rho| \sim U_1 \delta / \nu = \text{Re}(\delta/L), \quad (3.9)$$

where now  $\text{Re} = U_1 L / \nu \gg 1$ . Neglect of  $\nabla P_0$  is therefore justified if

$$\delta/L \ll \text{Re}^{-1} \ll 1, \quad (3.10)$$

a somewhat tighter requirement than (2.20).

Provided this condition is satisfied, the derivation of (3.7) is self-consistent, and it is apparent that the net effect of the Lorentz force within the skin of  $\Gamma$  is to provide an effective induced tangential stress

$$\tau_\Gamma = -\rho \nu \partial u / \partial \xi \Big|_{\xi=\infty} = \frac{1}{4} \rho \delta Q(x) \quad (3.11)$$

In the case of single-phase excitation,

$$Q(x) = (\mu_0 \rho)^{-1} \nabla |B_S|^2 \quad (3.12)$$

and from (3.1), neglecting surface tension effects, this becomes simply

$$Q(x) = \dot{g} - (g \cdot n) n = g_\Gamma, \quad (3.13)$$

the tangential projection of  $g$ , and the induced surface stress from (3.11) becomes

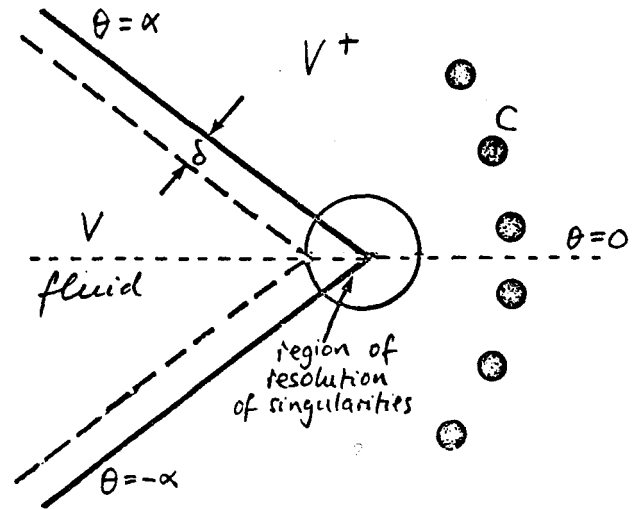
$$\tau_\Gamma = \frac{1}{4} \rho \delta g_\Gamma \quad (3.14)$$

Note that fluid particles on the surface are subject to viscous retardation as well as to gravitational acceleration  $g_\Gamma$ .

#### 4. THE BEHAVIOUR NEAR A SHARP CORNER ON S

Sharp corners are a feature of the rigid boundaries in many practical devices. For example, the typical induction furnace has a sharp corner where the cylindrical wall meets the horizontal base. Again, in the continuous casting problem, the melt is frequently extruded from a chamber of square cross-section within which it is stirred by a rotating field. The external potential field has to "turn round" a reflex angle at such corners and is unbounded in magnitude (in the high frequency limit). This means that effects originating near the corners may be of dominant importance in determining the character of the flow. These effects were touched on in the discussion of Ref. /11/; here we carry the analysis much further.

We shall suppose that the fluid is contained in the region  $\alpha < \theta < 2\pi - \alpha$  (Fig. 3), the boundaries  $\theta = \alpha, 2\pi - \alpha$

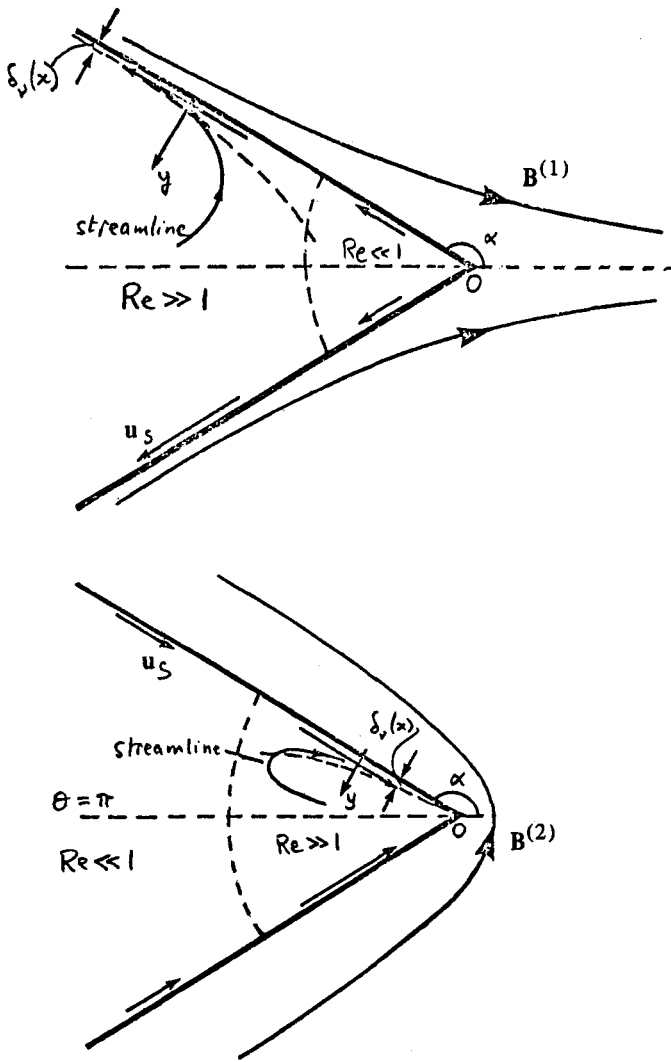


3 Corner configuration; singularities in  $B$  are resolved in region of overlap of electromagnetic skins on  $\theta = \pm\alpha$

being rigid insulators. The skin effect analysis of Section 2 will be valid on both boundaries except within a distance  $O(\delta)$  from the intersection where the two skins overlap; we shall ignore this minute region (in which any infinities in the magnetic field are obviously resolved).

There are three situations that need to be considered:

- (a) the case of a single-phase field  $B^{(1)}$  symmetric with respect to the corner bisector (Fig. 4a);
- (b) the case of a single-phase field  $B^{(2)}$  antisymmetric with respect to the corner bisector (Fig. 4b) — this is the case that arises in the induction furnace context;



4 (a) (above) single-phase symmetric field; (b) (below) single-phase antisymmetric field. Induced surface velocity  $u_s$  is as indicated by arrows.  $\delta_p(x)$  is boundary layer thickness,  $y$  normal boundary layer coordinate used in § 5. Streamlines are symmetric about  $\theta = \pi$

(c) the case of a rotating field, i.e. superposition of the fields  $B^{(1)}$  and  $B^{(2)}$  in quadrature.

Case (a)

The field potential  $\Phi^{(1)}$  in  $V^+$  is here given by

$$\Phi = \Phi_1 r^{\lambda_1} \cos \lambda_1 \theta \quad (4.1)$$

and the conditions  $B \cdot n = 0$  on  $\theta = \pm \alpha$  give immediately  $\lambda_1 = \pi/\alpha$ . The surface field on  $S$  is then

$$B_S^{(1)} = \partial \Phi^{(1)} / \partial r \Big|_{\theta = \pm \alpha} = -\Phi_1 \lambda_1 r^{\lambda_1 - 1} e_r \quad (4.2)$$

where  $e_r$  is a unit vector in the radial direction. Hence

$$|\nabla \Phi^{(1)}|^2 = 2\Phi_1^2 \lambda_1^2 (\lambda_1 - 1) r^{2\lambda_1 - 3} e_r \quad (4.3)$$

and so the induced surface velocity  $u_s$  is given from (2.21) by

$$u_s = Ar^m e_r \quad \text{on } \theta = \pm \alpha \quad (4.4)$$

where

$$A = \frac{\delta^2 \Phi_1^2}{8\mu_0 \rho \nu} \left( \frac{\pi}{\alpha} \right)^2 \left( \frac{\pi}{\alpha} - 1 \right) > 0 \quad (4.5)$$

and

$$m = 2\pi/\alpha - 3 \quad (4.6)$$

We may define a local Reynolds number

$$Re(r) = |u_s| r / \nu = Ar^{m+1} / \nu. \quad (4.7)$$

Since  $m+1 = 2\pi/\alpha - 2 > 0$  for all  $\alpha < \pi$ , it is evident that  $Re(r) \rightarrow 0$  as  $r \rightarrow 0$  and therefore that for sufficiently small  $r$ , a low Reynolds number analysis is valid. The streamfunction  $\psi(r, \theta)$  then satisfies the biharmonic equation

$$\nabla^4 \psi = 0 \quad (4.8)$$

and the boundary conditions are

$$\psi = 0, \quad r^{-1} \partial \psi / \partial \theta = Ar^m \quad \text{on } \theta = \pm \alpha \quad (4.9)$$

The particular integral proportional to  $r^{m+1}$  is

$$\psi = \frac{Ar^{m+1} \alpha [\sin(m-1)\alpha \sin(m+1)\theta]}{\alpha \sin 2(2\pi-3\alpha) - (2\pi-3\alpha) \sin 2\alpha} - \frac{Ar^{m+1} \alpha [\sin(m+1)\alpha \sin(m-1)\theta]}{\alpha \sin 2(2\pi-3\alpha) - (2\pi-3\alpha) \sin 2\alpha} \quad (4.10)$$

(and for  $\alpha > \pi/2$ , this certainly dominates over any complementary function since  $m+1 < 2$  - see Ref. /12/).

For large values of  $r$  for which  $Re(r) \gg 1$ , a boundary layer treatment is called for (see Section 5 below).

Case (b)

The potential for an antisymmetric field is

$$\Phi^{(2)} = \Phi_2 r^{\lambda_2} \sin \lambda_2 \theta \quad (4.11)$$

where now, from the conditions  $B \cdot n = 0$  on  $\theta = \pm \alpha$ .

$$\lambda_2 = \pi/2\alpha \quad (= \frac{1}{2}\lambda_1) \quad (4.12)$$

The surface field on  $S$  is now

$$B_S^{(2)} = \partial \Phi^{(2)} / \partial r \Big|_{\theta = \pm \alpha} e_r = \pm \Phi_2 \lambda_2 r^{\lambda_2 - 1} e_r \quad (\text{on } \theta = \pm \alpha) \quad (4.13)$$

For  $\pi/2 < \alpha < \pi$ , we have  $0 > \lambda_2 - 1 > -1/2$ , and the field  $B_S$  is evidently singular at  $r = 0$ ; of course, as pointed out above, this singularity is in fact resolved on the scale  $r = O(\delta)$ , so that  $|B_S^{(2)}|_{\max} \sim Q_2 (\pi/2\alpha) \delta^{(\pi/2\alpha - 1)}$ . The

singularity is "square-integrable" in the sense that the contribution to the magnetic energy

$$\int_0^R \int_{-\alpha}^{\alpha} (2\mu_0)^{-1} |\mathbf{B}^{(2)}|^2 r dr d\theta \quad (4.14)$$

from a neighbourhood  $0 < r < R$  of the corner is obviously finite, and is in fact  $O(R^{\pi/\alpha})$ .

As for case (a), we now find that

$$\nabla |\mathbf{B}_S^{(2)}|^2 = 2\Phi_2^2 \lambda_2^2 (\lambda_2 - 1) r^{2\lambda_2 - 3} \mathbf{e}_r \quad (4.15)$$

and the induced surface velocity is again given by

$$\mathbf{u}_S = A r^m \mathbf{e}_r \quad (4.16)$$

where now

$$A = \frac{\delta^2 \Phi_2^2}{8\mu_0 \rho \nu} \left(\frac{\pi}{2\alpha}\right)^2 \left(\frac{\pi}{2\alpha} - 1\right) \quad (4.17)$$

and

$$m = \pi/\alpha - 3 \quad (4.18)$$

For  $\alpha > \pi/2$ , we have  $m < -1$  and  $A < 0$ , so that the induced surface velocity is *towards* the corner, and  $\rightarrow \infty$  as  $r \rightarrow 0$ . The local Reynolds number is

$$\text{Re}(r) = |A| \nu^{-1} r^{\pi/\alpha - 2} \rightarrow \infty \quad \text{as } r \rightarrow 0 \quad (\alpha > \pi/2) \quad (4.19)$$

so that now a boundary-layer treatment is needed for *small*  $r$ . The low Reynolds number solution (4.10) is valid for *large* values of  $r$  such that  $\text{Re}(r) \ll 1$ . Thus the situation in case (b) is just the converse of that of case (a) (see Figs. 4a, b).

*Case (c)*

When the fields  $\mathbf{B}_S^{(1)}$ ,  $\mathbf{B}_S^{(2)}$  are present simultaneously and in quadrature (thus representing a rotating field in the neighbourhood of the corner), we have the two contributions (4.3) and (4.15) to  $\mathbf{Q}(\mathbf{x})$  and also the contribution

$$\text{Im} \mathbf{B}_S^* (\nabla \cdot \mathbf{B}_S) = \mp \Phi_1 \Phi_2 \frac{\pi^3}{4\alpha^3} r^{3\pi/(2\alpha) - 3} \mathbf{e}_r \quad \text{on } \theta = \pm \alpha \quad (4.20)$$

Hence we find for the induced surface velocity

$$\mathbf{u}_S = \frac{\delta^2 \pi^2}{64\nu\alpha^2} r^{\pi/\alpha - 3} \left[ -2\Phi_2^2 \left(1 - \frac{\pi}{2\alpha}\right) \mp \Phi_1 \Phi_2 \frac{\pi}{\alpha} r^{\pi/2\alpha} + 8\Phi_1^2 \left(\frac{\pi}{\alpha} - 1\right) r^{\pi/\alpha} \right] \mathbf{e}_r \quad \text{on } \theta = \pm \alpha \quad (4.21)$$

Of the three contributions to  $\mathbf{u}_S$ , the first dominates for small  $r$  and the last dominates for large  $r$ ; these are the terms arising from the  $\nabla |\mathbf{B}_S|^2$  contributions which

generate symmetric flows. The second term (with the  $\mp$ ) is comparable with the other two in the transition region and here it generates the antisymmetric ingredient of the flow which is responsible for carrying the fluid round the corner in the same sense as the rotation of the field (see Fig. 5).

## 5. HIGH REYNOLDS NUMBER FLOW FOR SINGLE PHASE EXCITATION

We have already noted that in case (a) above a high Reynolds number flow is generated *far* from the corner, while in case (b) a high Reynolds number flow is generated *near* the corner. In both cases

$$\mathbf{u}_S = A r^m \mathbf{e}_r \quad \text{on } \theta = \pm \alpha \quad (5.1)$$

with

$$\left. \begin{aligned} A > 0, m + 1 > 0 & \quad \text{in case (a)} \\ A < 0, m + 1 < 0 & \quad \text{in case (b)} \end{aligned} \right\} \quad (5.2)$$

This is a situation which lends itself to boundary-layer analysis. Let  $Ox$  be directed along the boundary  $\theta = \alpha$ , and  $Oy$  normal to it and into the fluid (see Fig. 4); then the boundary-layer equation for the stream-function  $\psi(x, y)$  is

$$\psi_y \psi_{xy} - \psi_x \psi_{yy} = \nu \psi_{yyy} \quad (5.3)$$

and the boundary conditions are

$$\left. \begin{aligned} \psi = 0, \quad \psi_y = Ax^m \quad \text{on } y = 0 \\ \psi_y \rightarrow 0 \quad \text{as } y \rightarrow \infty \end{aligned} \right\} \quad (5.4)$$

Here we are supposing that there is no pressure gradient outside the boundary layer, as seems plausible for the corner configuration. The standard similarity arguments of boundary-layer theory (Ref. /13/, Section 5.9) imply that

$$\psi = (\nu |A| x^{m+1})^{1/2} f(\eta) \quad \text{where } \eta = (|A| x^{m+1} \nu^{-1})^{1/2} y \quad (5.5)$$

and equation (5.3) then reduces to

$$f''' + \frac{1}{2}(m+1)ff'' - mf'^2 = 0 \quad (5.6)$$

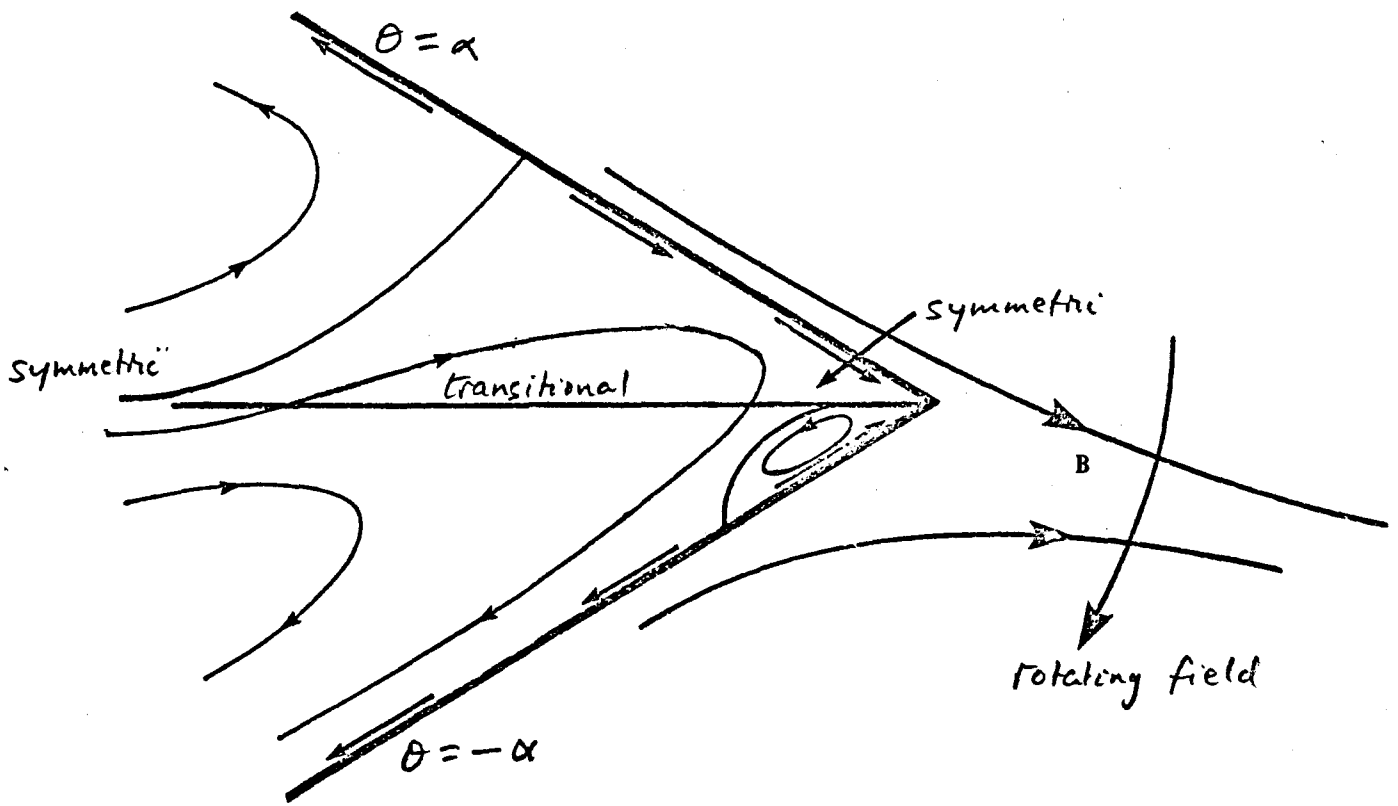
with boundary conditions

$$f(0) = 0, \quad f'(\infty) = 0 \quad (5.7)$$

and

$$f'(0) = \begin{cases} +1 & \text{(case (a))} \\ -1 & \text{(case (b))} \end{cases} \quad (5.8)$$

Equation (5.6) is similar to (but not identical with) the



5 Induced surface velocity and resulting streamline pattern under action of rotating field at sharp corner

Falkner-Skan equation, and it may be integrated numerically.

For case (a), the form of  $f'(\eta)$  for various values of  $m$  in the range  $1 \geq m > -\frac{1}{2}$  is shown in Fig. 6a. Note the particular exact solutions

$$\left. \begin{aligned} f(\eta) &= 1 - e^{-\eta} & \text{when } m &= 1 \\ f(\eta) &= \sqrt{6} \operatorname{th}(\eta/\sqrt{6}), & \text{when } m &= -1/3 \end{aligned} \right\} \quad (5.9)$$

which check with the computed curves. When  $m = -1/3$ ,  $f''(\eta) = 0$ , and so the wall stress vanishes. For  $-1/2 < m < -1/3$ , there is an "overshoot" of tangential velocity near the wall, which becomes large as  $m \rightarrow -\frac{1}{2}$ . For  $m \leq -\frac{1}{2}$ , no solution of (5.6)–(5.7) exists satisfying  $f'(0) = 1$ . The values  $m = -1/3, -1/2$  correspond to  $\alpha = 3\pi/4, 4\pi/5$  respectively, so that, as wedge angle  $2\pi - 2\alpha$  containing the fluid decreases from  $\pi/2$  to  $2\pi/5$ , this anomalous type of boundary-layer behaviour is to be expected; and when the wedge angle is less than  $2\pi/5$ , these results would suggest that the wall acceleration implied by (5.4) is insufficient to sustain a self-similar boundary-layer solution, and the boundary-layer approximation is then presumably no longer valid.

For case (b), the solutions of (5.6)–(5.8) appear to be quite regular, and are shown in Fig. (6b) for values of  $m$  in the range  $-1 \leq m \leq -2$  (i.e. from (4.18),  $\pi/2 \leq \alpha \leq \pi$ ). In this case, there is no indication of any breakdown in boundary-layer theory when the angle  $2\alpha$  is reflex (as in Fig. 4b). Note that, in both cases (a) and (b), the boundary-layer thickness

$$\delta_\nu(x) = (\nu/|A|)^{1/2} x^{1/2(1-m)} \quad (5.10)$$

decreases in the direction of  $u_s$ , in a manner characteristic of accelerating flows.

The normal velocity at the outer edge of the boundary layer is given (in case (a) or case (b)) by

$$\begin{aligned} V(x) &= \lim_{y \rightarrow \infty} \left( -\frac{\partial \psi}{\partial x} \right) = \\ &= -\frac{1}{2}(m+1)(\nu|A|)^{1/2} x^{1/2(m-1)} f(\infty) \end{aligned} \quad (5.11)$$

Returning to polar coordinates  $(r, \theta)$ , the potential flow  $u = \nabla \varphi$  in the core which matches with this velocity is

$$\varphi = \varphi_0 r^{1/2(m+1)} \cos 1/2(m+1)\theta \quad (5.12)$$

where

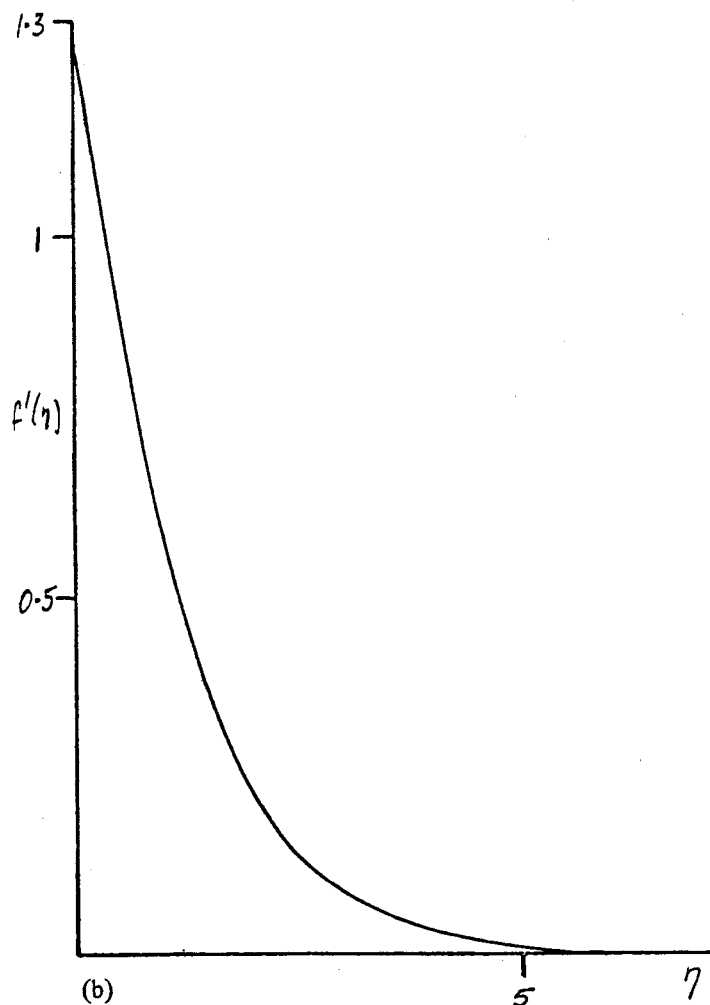
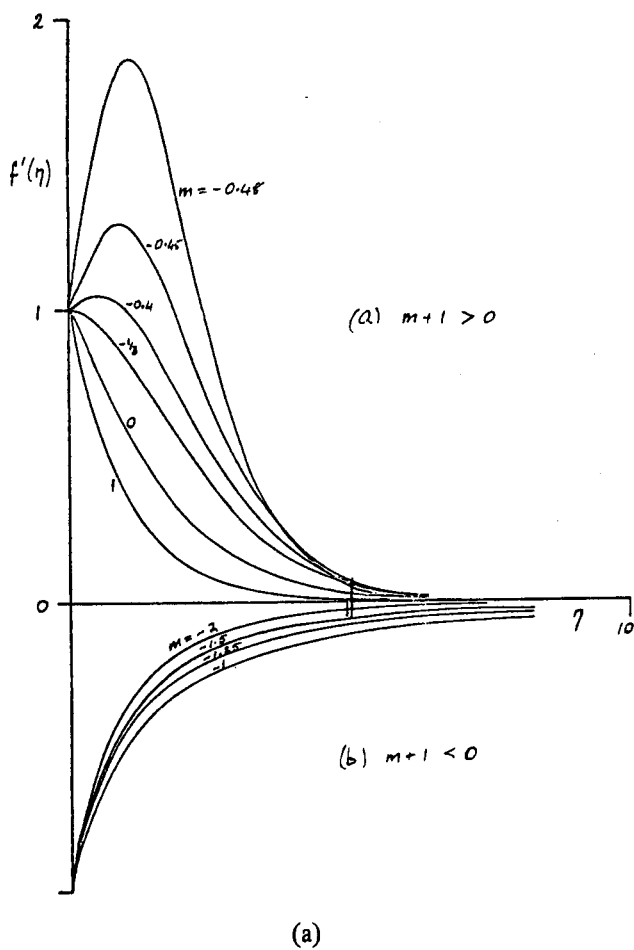
$$\varphi_0 \sin 1/2(m+1)\alpha = (\nu|A|)^{1/2} f(\infty) \quad (5.13)$$

The associated tangential velocity  $(\partial \varphi / \partial r)_{\theta = \pm \alpha}$  is small compared with  $|u_s|$  in the range of  $r$  for which  $\operatorname{Re}(r) \gg 1$ .

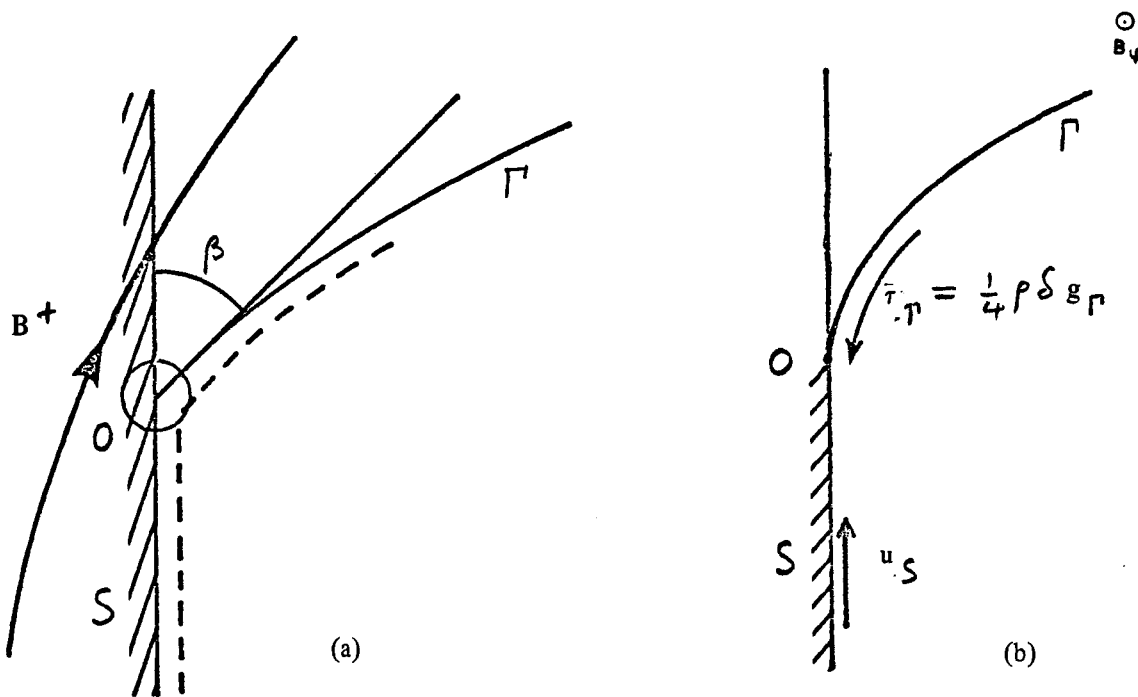
The streamline patterns which may be inferred from these solutions have been included in Figs. 4a, b.

6. INTERSECTION OF A FREE SURFACE AND A RIGID BOUNDARY

We turn now to some considerations involving free surface behaviour. Consider first conditions near a contact



6 Computed form of  $f'(\eta)$ ; (a) (above left) for problem (5.6)–(5.8) for case (a) with  $1 \geq m > -0.5$ ; (b) (below left) for case (b) with  $-1 \geq m \geq -2$ ; (c) (right) for free surface problem (7.5)



7 Intersection of free surface  $\Gamma$  and rigid boundary  $S$ ; situation as sketched in (a) (left) is impossible, because magnetic pressure would be unbounded in any neighbourhood of  $O$ , and condition (3.1) could not then be satisfied. Cusped configuration, as sketched in (b) (right) must occur. Interior flow is then predominantly driven by surface stress  $\tau_\Gamma$

line of a free surface  $\Gamma$  and a rigid boundary  $S$  (Fig. 7a). This situation arises in problems of partial levitation, when part of the fluid is supported by a solid boundary. It also arises in the induction furnace context (although here the frequencies employed are generally not large enough for validity of the present analysis).

On scales large compared with the skin thickness  $\delta$ , the angle of intersection  $\beta$  of  $\Gamma$  and  $S$  cannot in general be nonzero — i.e. the situation envisaged in Fig. 7a is in fact impossible — because the magnetic pressure on  $\Gamma$  would then be unbounded in the neighbourhood of  $O$ , in such a way that the normal stress condition (3.1) could not be satisfied. The magnetic pressure would tend to depress the free surface until a cusped configuration is established, as shown in Fig. 7b.

The induced surface stress on  $\Gamma$  is given by (3.14), and this stress determines the nature of the interior flow (the induced surface velocity on  $S$  being less important here). The actual shape of the surface  $\Gamma$  near the contact line presents an intriguing problem which has not yet been solved.

## 7. DISTORTION OF A FREE SURFACE BY A SYMMETRIC FIELD

If the field  $B^+$  is produced by two equal and opposite line currents placed above a free surface as in Fig. 8a, then it is clear that the magnetic pressure on the surface will cause a symmetric distortion. As the current strength is increased, a sharp crest may appear as indicated in Fig. 8b, in some respects similar to the sharp crest that appears under a progressive gravity wave of maximum height (Ref. /13/, p. 506, problem 3b). As in this well-known context, the angle at the crest must be  $2\pi/3$  (so that  $\alpha = 2\pi/3$  also); the surface field  $B_S$  is then given locally (see equation (4.2)) by  $B_S \sim -\frac{3}{2} \Phi r^{1/2} e_r$ , so that the magnetic pressure  $(9/8\mu_0)\Phi^2 r$  can be compensated by the term  $\rho g \cdot x = -\frac{1}{2}\rho g r$  in (3.1).

From (3.14), the induced surface stress is

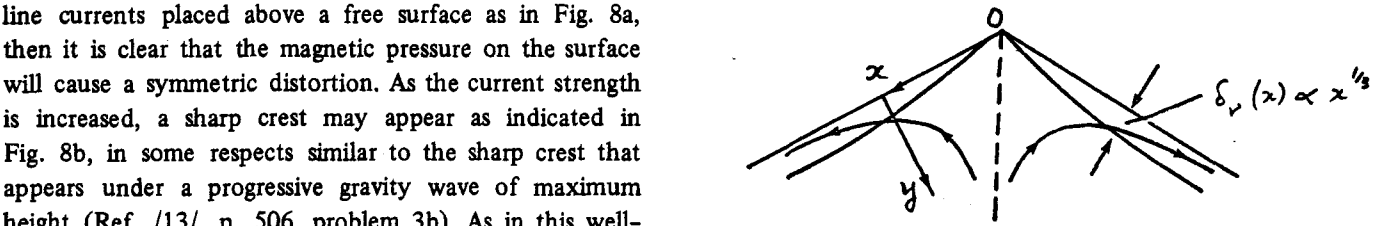
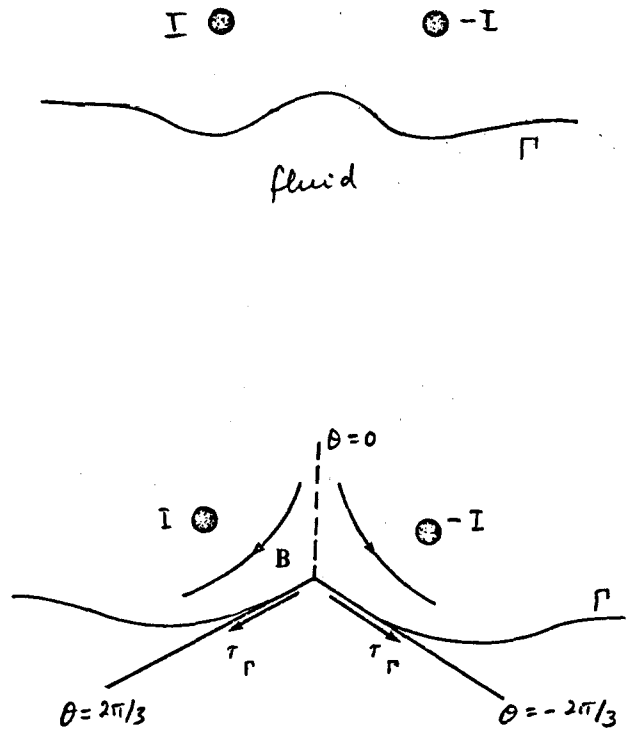
$$\tau_\Gamma = \frac{1}{8} \rho \delta g e_r \quad (7.1)$$

down both surfaces away from the crest  $O$ . Equivalently, using boundary layer variables  $(x, y)$  as shown in Fig. 8c, we have an induced surface shear

$$(\partial u / \partial y)_{y=0} = -S = -(\rho \nu)^{-1} \tau_\Gamma = -\delta g / 8 \nu \quad (7.2)$$

on both  $\theta = \pm\alpha$ . The boundary-layer problem (cf. equations (5.3) and (5.4)) is then

$$\left. \begin{aligned} \psi_y \psi_{xy} - \psi_x \psi_{yy} &= \nu \psi_{yyy} \\ \psi &= 0, \quad \psi_{yy} = -S \quad \text{on } y=0 \\ \psi_y &= 0 \quad \text{as } y \rightarrow \infty \end{aligned} \right\} \quad (7.3)$$



8 (a) (top) Distortion of free surface by magnetic pressure due to parallel line currents; (b) (middle) formation of sharp crest and associated surface stress; (c) boundary-layer structure of resulting flow

and dimensional arguments lead to the similarity solution

$$\psi = (x\nu S^{1/2})^{2/3} f(\eta) \quad \eta = (S/x\nu)^{1/3} y \quad (7.4)$$

where  $(m = 1/3$  in equation (5.6))

$$\left. \begin{aligned} f''' + \frac{2}{3} f f'' - \frac{1}{3} f'^2 &= 0 \\ f(0) = 0, \quad f''(0) = -1, \quad f'(\infty) &= 0 \end{aligned} \right\} \quad (7.5)$$

A well-behaved solution exists satisfying  $f'(\eta) > 0$  for all  $\eta$  (see Figure 6c). The surface velocity is given by

$$u_S = \partial \psi / \partial y |_{y=0} = \frac{1}{4} x^{1/3} (\delta g)^{2/3} \nu^{-1/3} f'(0) \quad (7.6)$$

The core flow which matches with this is  $u = \nabla\varphi$  where

$$\varphi = (\nu S^{1/2} r)^{2/3} f(\infty) \frac{\sin^{2/3} \theta}{\cos(4\pi/9)}$$

$$(\alpha < \theta < 2\pi - \alpha) \quad (7.7)$$

This has an associated tangential velocity

$$u'_S = \partial\varphi/\partial r |_{\theta=\alpha, 2\pi-\alpha} =$$

$$= \pm \frac{2}{3} (\nu S^{1/2})^{2/3} r^{-1/3} f(\infty) \tan(4\pi/9)$$

and for consistency we must require that  $|u'_S| \ll |u_S|$ , a condition that is satisfied provided

$$r \gg \lambda (\nu/S)^{1/2} \quad (7.8)$$

This is again just the condition that the local Reynolds number  $ru_S(r)/\nu$  be large. The local structure of the flow is as indicated (on an expanded scale) in Fig. 8c.

#### ACKNOWLEDGEMENTS

I am most grateful to Dr. B.R. Duffy who found the exact solutions (5.9) of the boundary layer problem (5.6) –

(5.8) and who computed the solution curves of Fig. 6; and to Dr. A.D. Sneyd for initial discussions of the free surface problem of Section 7.

#### REFERENCES

1. E.D. TARAPORE and J.W. EVANS, *Metal Trans.*, 1976, 7B, 343-351.
2. R. MOREAU, "MHD-Flows and Turbulence II", ed. H. Branover and A. Yakhot, 1980, Israel University Press, Jerusalem, pp. 65-82.
3. J.A. SHERCLIFF, *Proc. Roy. Soc.*, 1981, A375, 455-473.
4. J. MESTEL, *J. Fluid Mech.*, 1982, 117, 27.
5. A.D. SNEYD and H.K. MOFFATT, *J. Fluid Mech.*, 1982, 117, 45-70.
6. D.J. HAYES, M.R. BAUM and M.R. HOBDELL, *J. Br. Nucl. Energy Soc.*, 1971, 10, 93-98.
7. T. ROBINSON, *J. Fluid Mech.*, 1973, 60, 641-664.
8. A.B. KAPUSTA, *Mag. Gidrod.*, 1969, 5, 117-120.
9. H.K. MOFFATT, *J. Fluid Mech.*, 1965, 22, 521-528.
10. H.K. MOFFATT, "MHD-Flows and Turbulence II", ed. H. Branover and A. Yakhot, 1980, Israel University Press, Jerusalem, pp. 45-64.
11. H.K. MOFFATT, *ZAMM*, 1978, 58, 65-71.
12. H.K. MOFFATT and B.R. DUFFY, *J. Fluid Mech.*, 1980, 96, 299-313.
13. G.K. BATCHELOR, "Introduction to Fluid Dynamics", 1967, Cambridge University Press.
14. A.D. SNEYD, *J. Fluid Mech.*, 1979, 92, 35-51.